

The growth of ZnMgO alloy films for deep ultraviolet detection

This article has been downloaded from IOPscience. Please scroll down to see the full text article.

2008 J. Phys. D: Appl. Phys. 41 125104

(<http://iopscience.iop.org/0022-3727/41/12/125104>)

[The Table of Contents](#) and [more related content](#) is available

Download details:

IP Address: 155.69.4.4

The article was downloaded on 29/10/2008 at 08:40

Please note that [terms and conditions apply](#).

The growth of ZnMgO alloy films for deep ultraviolet detection

K W Liu^{1,2}, D Z Shen¹, C X Shan¹, J Y Zhang¹, D Y Jiang¹, Y M Zhao¹,
B Yao¹ and D X Zhao¹

¹ Key Laboratory of Excited State Processes, Changchun Institute of Optics, Fine Mechanics and Physics, Chinese Academy of Sciences, Changchun 130033, People's Republic of China

² Graduate School of the Chinese Academy of Sciences, Beijing 100049, People's Republic of China

E-mail: zhangjy53@yahoo.com.cn and liukewei23@sohu.com

Received 24 February 2008, in final form 1 April 2008

Published 29 May 2008

Online at stacks.iop.org/JPhysD/41/125104

Abstract

ZnMgO films are prepared by RF magnetron sputtering using a composite target and the Mg composition of the samples can be controlled easily even at a high growth temperature. The metal–semiconductor–metal photodetector based on the wurtzite $\text{Zn}_{0.6}\text{Mg}_{0.4}\text{O}$ film exhibits a very low dark current (5 pA at $|V_{\text{bias}}| = 3$ V) and a high UV/visible rejection ratio (more than three orders of magnitude). The peak responsivity of the photodetector is at around 270 nm and a very sharp cutoff wavelength is at a wavelength of about 295 nm corresponding to the absorption edge of the $\text{Zn}_{0.6}\text{Mg}_{0.4}\text{O}$ film.

(Some figures in this article are in colour only in the electronic version)

ZnO based materials have attracted considerable attention in the last few years for their potential applications in optoelectronic devices operating in the UV region [1–3]. As a direct band gap material, ZnMgO is a strong candidate in photodetectors for its high absorption coefficient and abrupt absorption edge. Meanwhile, ZnO films prepared on lattice-matched substrates have a relatively low dislocation density and very high transmittance in the visible region. Furthermore, ZnMgO materials have high radiation hardness [8] and tunable band-gap energy (3.3–7.8 eV) [5–7]. These properties are crucial for practical high-performance optoelectronic devices. Solar or visible-blind $\text{Zn}_{1-x}\text{Mg}_x\text{O}$ photodetectors have been fabricated on sapphire [4, 9], glass [4] and silicon substrates [10, 11]. Photodetectors based on $\text{Mg}_{0.68}\text{Zn}_{0.32}\text{O}/\text{SrTiO}_3/\text{Si}$ show peak photoresponsivity at 225 nm, but their UV/visible rejection ratio is only one order of magnitude [11]. Prototype $\text{Zn}_{1-x}\text{Mg}_x\text{O}$ UV photodetectors with different Mg contents showed high photoresponsivities and sharp cutoffs at ~ 375 nm, ~ 350 nm, ~ 315 nm and ~ 300 nm for the x values of 0, 0.10, 0.26 and 0.34, respectively [10]. Takeuchi *et al* have fabricated monolithic multichannel ultraviolet detector arrays and the peak response wavelength shifts with the increase in the Mg mole fraction from 380 nm for ZnO to 288 nm for wurtzite $\text{Mg}_{0.38}\text{Zn}_{0.62}\text{O}$ [12]. In our previous work, the metal–semiconductor–metal (MSM) structured $\text{Mg}_{0.2}\text{Zn}_{0.8}\text{O}$ detector

and the $\text{Mg}_{0.24}\text{Zn}_{0.76}\text{O}$ homojunction photodiode have been fabricated with a cutoff wavelength of 350 nm and 345 nm, respectively [13, 14]. However, no reports that the cutoff wavelength (the peak response wavelength) is shorter than 300 nm (288 nm) can be found for the photodetectors based on wurtzite ZnMgO. Furthermore, since Mg and Zn species have different vapour pressures, Mg composition in the deposition is difficult to control and usually larger than that in the precursor target using pulsed laser deposition (PLD) [7].

In this paper, ZnMgO films were prepared by radio frequency (RF) magnetron sputtering using a composite target and the Mg composition in the samples can be controlled easily. The Mg concentrations in the $\text{Zn}_{1-x}\text{Mg}_x\text{O}$ films were determined by energy dispersive spectroscopy (EDS) (GENESIS 2000 XMS 60S) attached to a scanning electron microscope (HICACHI, S-4800). The $\text{Zn}_{0.6}\text{Mg}_{0.4}\text{O}$ MSM photodetector has been fabricated. The peak responsivity was located at around 270 nm and a very sharp cutoff wavelength at about 295 nm. Furthermore, the dark current of the $\text{Zn}_{0.6}\text{Mg}_{0.4}\text{O}$ MSM photodetector was lower than 200 pA below 95 V.

ZnMgO thin films were prepared on quartz substrates using an RF magnetron sputtering technique. A high-purity ZnMgO ceramic plate was placed on a Zn metal disc, which were employed as the precursor target. The sketch of the

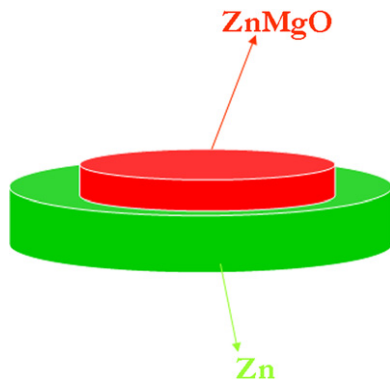


Figure 1. Schematic diagram of the composite ZnMgO–Zn target.

ZnMgO–Zn composite target is shown in figure 1. The Zn disc was 90 mm in diameter, and the ZnMgO ceramic plate was 60 mm. The quartz substrates were cleaned using acetone and ethanol for 5 min in an ultrasonic bath, followed by a de-ionized water rinse. Quartz substrates were placed on the sample holder which is parallel to the target. The distance between the substrate and the target was 75 mm. The chamber was pumped down to 10^{-4} Pa by a turbo molecular pump. The pressure in the chamber was kept at 1.0 Pa during the film growth. The RF power was kept at 100 W and the substrate temperature at 400 °C during deposition. High-purity argon and oxygen (99.999%) with a flow ratio of 7 : 1 acted as the ambient gas in the sputtering process. The Mg/Zn atomic ratio in the films was adjusted by changing the composition of the ZnMgO ceramic. Compared with the conventional single ceramic target, our composite target could easily control the Mg/Zn atomic ratio in the films. This phenomenon can be explained by the fact that a cover of Zn atoms was formed around the ZnMgO ceramic by a Zn metal disc during sputtering, and this cover can maintain the Mg/Zn atomic ratio in the films corresponding well to the ZnMgO ceramic even at a high substrate temperature. Therefore, in our work, the composition of the ZnMgO films was insensitive to the growth temperature and can be controlled easily.

Figure 2 shows the ultraviolet–visible absorption spectra of $Zn_{1-x}Mg_xO$ films with different x values. The absorption edge of pure ZnO was at about 385 nm, while that of $Zn_{0.6}Mg_{0.4}O$ at about 295 nm. In this region, the transmission edge shifts by a total of 90 nm at the rate of about 18 nm for every 8 mol% increase in Mg. The phase separation was evident for compositions whose absorption edge was between 290 and 240 nm. In this region (shaded in the figure 2), double absorption edges for each sample appeared, which may come from the cubic and the wurtzite phase [12, 15]. Beyond the phase separated region, the bandgap of cubic $Zn_{1-x}Mg_xO$ could be tuned again until the composition of $Zn_{1-x}Mg_xO$ approaches pure MgO.

Figure 3 showed the transmission and absorption spectrum of the $Zn_{0.6}Mg_{0.4}O$ film on quartz. It was clear from the transmission spectrum that the sample had more than 80% transmission in the visible region. The absorption spectrum showed a strong absorption at 295 nm corresponding to a band gap of 4.2 eV. The inset of figure 3 showed the x-ray diffraction

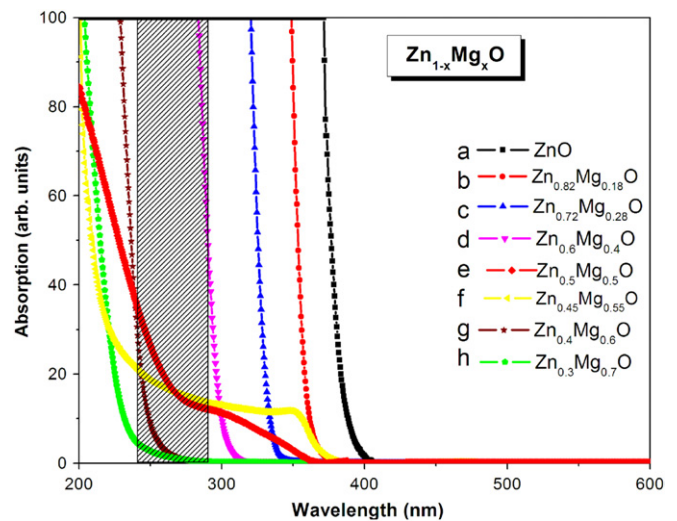


Figure 2. UV–visible absorption spectra of $Zn_{1-x}Mg_xO$ films on quartz substrates with different Mg contents: a—ZnO, b— $Zn_{0.82}Mg_{0.18}O$, c— $Zn_{0.72}Mg_{0.28}O$, d— $Zn_{0.6}Mg_{0.4}O$, e— $Zn_{0.5}Mg_{0.5}O$, f— $Zn_{0.45}Mg_{0.55}O$, g— $Zn_{0.4}Mg_{0.6}O$ and h— $Zn_{0.3}Mg_{0.7}O$.

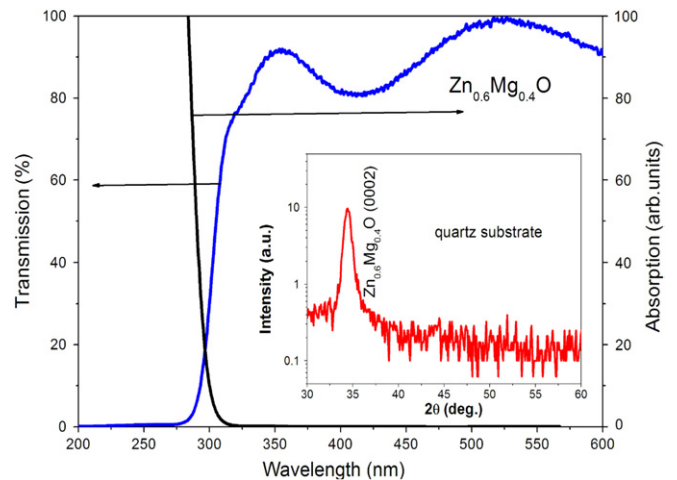


Figure 3. UV–visible absorption and transmission spectrum of the $Zn_{0.6}Mg_{0.4}O$ film and the inset shows the x-ray diffraction pattern.

pattern of the $Zn_{0.6}Mg_{0.4}O$ film. The appearance of only the (0002) diffraction peak indicated that the film is highly c -axis oriented and corresponds to the hexagonal wurtzite structure of ZnMgO. No other phase can be observed.

The photodetectors based on the $Zn_{0.6}Mg_{0.4}O$ film with the metal–semiconductor–metal structure were fabricated using standard semiconductor fabrication techniques. The interdigital metal electrodes, which were defined on a 200 nm Au layer by conventional UV photolithography and the lift-off procedure, are 500 μm long and 5 μm wide, with a 5 μm gap (shown in the left-top inset of figure 4). The typical I – V characteristics of the $Zn_{0.6}Mg_{0.4}O$ film based MSM detector were measured by a semiconductor analyzer (Keithley 4200), as shown in figure 4. The device exhibited a very low dark current (lower than 200 pA for $|V_{\text{bias}}| < 95$ V), and it was not broken down even when the applied bias voltage is larger than 100 V. The dark and photoilluminated I – V characteristics of the $Zn_{0.6}Mg_{0.4}O$ MSM planar device are shown in the right

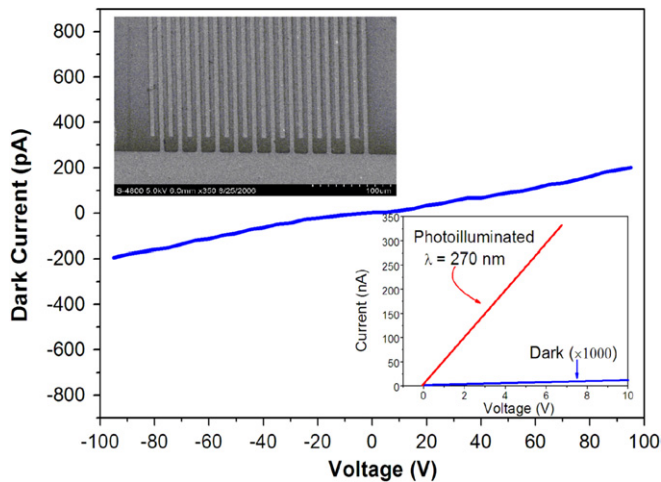


Figure 4. Dark current versus applied bias of the $\text{Zn}_{0.6}\text{Mg}_{0.4}\text{O}$ MSM photodetector. The left-top inset shows the microscope image of the interdigitated electrode configuration of our MSM device. The right inset shows the I - V curves of the device (photoilluminated at 270 nm and dark).

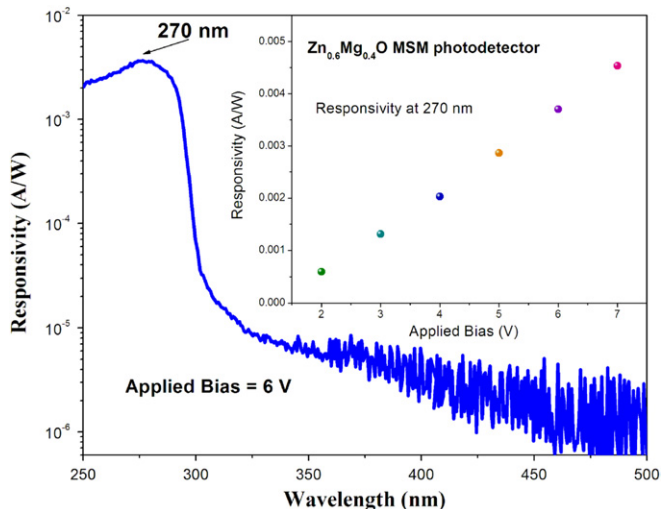


Figure 5. The spectral response of the $\text{Zn}_{0.6}\text{Mg}_{0.4}\text{O}$ UV detector with a $5\ \mu\text{m}$ finger pitch biased at 6 V. The inset shows the responsivity at 270 nm as a function of reverse bias.

inset of figure 4. The wavelength of the illuminated light is 270 nm. Under 3 V bias, the dark current and photocurrent is 5 pA and 150 nA, respectively.

The spectral responses have been measured at different bias voltages, and an example is shown in figure 5. The device showed a peak response at about 270 nm, which was in the solar-blind UV region. The cutoff wavelength is at about 295 nm corresponding to the absorption edge of the $\text{Zn}_{0.6}\text{Mg}_{0.4}\text{O}$ film. The UV/visible rejection ratio is more than three orders of magnitude. Furthermore, the detector

responsivity at 270 nm increases almost linearly with the bias voltage, as illustrated in the inset of figure 5.

In summary, we have prepared ZnMgO films on a quartz substrate by RF magnetron sputtering using a composite target and the Mg composition of the samples can be controlled easily, even at a high growth temperature. The MSM deep ultraviolet photodetector based on the wurtzite $\text{Zn}_{0.6}\text{Mg}_{0.4}\text{O}$ film exhibits a peak responsivity at 270 nm and a very sharp cutoff wavelength at around 295 nm. The $\text{Zn}_{0.6}\text{Mg}_{0.4}\text{O}$ MSM UV detector exhibits a very low dark current, a high breakdown voltage and a high UV to visible rejection ratio.

Acknowledgments

This work is supported by the Key Project of National Natural Science Foundation of China under Grant Nos 60336020 and 50532050, the '973' program under Grant Nos 2008CB317105 and 2006CB604906 and the Key Project of Chinese Academy of Science under Grant No kjcx3.syw.w01.

References

- [1] Look D C 2001 *Mater. Sci. Eng. B* **80** 383
- [2] Pearton S J, Norton D P, Ip K, Heo Y W and Steiner T 2004 *J. Vac. Sci. Technol. B* **22** 932
- [3] Mandalapu L J, Yang Z, Xiu F X, Zhao D T and Liu J L 2006 *Appl. Phys. Lett.* **88** 092103
- [4] Hullavarad S S, Dhar S, Varughese B, Takeuchi I, Venkatesan T and Vispute R D 2005 *J. Vac. Sci. Technol. A* **23** 982
- [5] Narayan J, Sharma A K, Kvit A, Jin C, Muth J F and Holland O W 2002 *Solid State Commun.* **121** 9
- [6] Ohtomo A, Kawasaki M, Koida T, Masubuchi K, Koinuma H, Sakurai Y, Yoshida Y, Yasuda T and Segawa Y 1998 *Appl. Phys. Lett.* **72** 2466
- [7] Choopun S, Vispute R D, Yang W, Sharma R P, Venkatesan T and Shen H 2002 *Appl. Phys. Lett.* **80** 1529
- [8] Auret F D, Goodman S A, Hayes M, Legodi M J, van Laarhoven H A and Look D C 2001 *Appl. Phys. Lett.* **79** 3074
- [9] Yang W, Vispute R D, Choopun S, Sharma R P, Venkatesan T and Shen H 2001 *Appl. Phys. Lett.* **78** 2787
- [10] Koike K, Hama K, Nakashima I, Takada G-Y, Ogata K-I, Sasa S, Inoue M and Yano M 2005 *J. Cryst. Growth* **278** 288
- [11] Yang W, Hullavarad S S, Nagaraj B, Takeuchi I, Sharma R P, Venkatesan T, Vispute R D and Shen H 2003 *Appl. Phys. Lett.* **82** 3424
- [12] Takeuchi I, Yang W, Chang K-S, Aronova M A, Venkatesan T, Vispute R D and Bendersky L A 2003 *J. Appl. Phys.* **94** 7336
- [13] Liu K W, Zhang J Y, Ma J G, Jiang D Y, Lu Y M, Yao B, Li B H, Zhao D X, Zhang Z Z and Shen D Z 2007 *J. Phys. D: Appl. Phys.* **40** 2765
- [14] Liu K W, Shen D Z, Shan C X, Zhang J Y, Yao B, Zhao D X, Lu Y M and Fan X W 2007 *Appl. Phys. Lett.* **91** 201106
- [15] Sanjeev Kumar, Vinay Gupte and Sreenivas K 2006 *J. Phys.: Condens. Matter* **18** 3343